Journal of Achievements in Materials and Manufacturing Engineering
VOLUME 17
ISSUE 1-2
July-August
2006

The effect of cast Al-Si-Cu alloy solidification rate on alloy thermal characteristics

L.A. Dobrzański [a,*], R. Maniara [a], J.H. Sokolowski [b]
[a] Division of, Materials Processing Technology and Computer Techniques in Materials Science, Institute of Engineering Materials and Biomaterials, Silesian University of Technology, ul. Konarskiego 18a, 44-100 Gliwice, Poland
[b] Industrial Research Chair in Light Metals Casting Technology, University of Windsor, 401 Sunset Ave.,N9B 3P4, Windsor, Ontario, Canada
* Corresponding author: E-mail address: leszek.dobrzanski@polsl.pl

Received 15.03.2006; accepted in revised form 30.04.2006

Methodology of research

ABSTRACT

Purpose: In the metal casting industry, an improvement of component quality depends mainly on better control over the production parameters. Thus, a thermal analysis cooling curve of the alloy is used for process control in the aluminum casting industry. In this work effect of cooling rate on the size of the grains, SDAS, size of the β precipitation and thermal characteristic results of AC AlSi9Cu cast alloy have been described. The solidification process was studied using the cooling curve and crystallization curve at solidification rate ranging from 0,16 $^{o}Cs^{-1}$ up to 1,04 $^{o}Cs^{-1}$
Design/methodology/approach: The experimental alloy used in this investigation was prepared by mixing the ACAlSi5Cu commercial alloys and two master alloys AlSi49 and AlCu55. Thermal analysis tests were conducted using the UMSA Technology Platform. Cooling curve thermal analysis was performed on all samples using high sensitivity thermocouples of K type. Data were acquired by a high speed data acquisition system linked to a PC computer. Each chilled sample was sectioned horizontally where the tip of the thermocouple was located and it was prepared by standard grinding and polishing procedures. Optical microscopy was used to characterize the microstructure and intermetallic phases. Secondary Dendrite Arm Spacing measurements were carried out using an Leica Q-WinTM image analyzer.
Findings: Increasing the cooling rate increases significantly the liquidus temperature, nucleation undercooling temperature, solidification range and decreases the recalescence undercooling temperature. Increasing cooling rate refines all microstructural features.
Research limitations/implications: This paper presents results for one alloy - AC AlSi9Cu only, for the assessment of the Silicon Modification Level didn't include the arrangement of a Si crystal in a matrix.
Originality/value: Original value of the work is applied the artificial intelligence for the assessment of the Silicon Modification Level.
Keywords: Quantitative metallography; Image analysis; Thermal analysis; Thermal characteristic

1. Introduction

The AC AlSi9Cu aluminum alloy has been widely used in the automotive industry due to its good casting characteristics and mechanical properties. In designing cast automotive parts, it is important to have an intimate knowledge of how alloy solidifies at different cross sections of the cast part and how this influences mechanical properties. This knowledge enables the designer to

ensure that the casting will achieve the desired properties for its intended application.

High purity AlSiCu hypoeutectic alloys exhibit three main solidification reactions during the solidification process, starting with the formation of aluminum dendrites (liquidus) followed by the development of two main eutectic phases. The presence of alloying and impurity elements such as: Cu, Mg, Mn, Fe leads to more complex constituents (including intermetallic) that are characterized by metallographic techniques. Bäckerud et al. [6, 8, 9, 10] identified the reactions in AC AlSiXCuX, (3XX) alloys and listed four solid state phases, Table 1.

Table 1
Reactions occurring during the solidification of the AC AlSiXCuX, (3XX) alloys according to [6, 8, 9, 10]

No	Reaction	Temperature [ºC]
1	Development of dendritic network	620÷580
2	$L \rightarrow \alpha + \beta + AlFe_5Si$	570÷555
3	$L \rightarrow \alpha + \beta + Al_8FeMg_3Si_6 + Mg_2Si$	540÷500
4	$L \rightarrow \alpha + Al_2Cu + \beta + Al_5Cu_2Mg_8Si_6$	500÷470

The solidification path for AC AlSiXCuX, (3XX) alloys can be described as fallows [6, 8, 10]:

1. A primary α-aluminum dendrite network forms between 620÷580 ºC. The exact temperature depends mainly on the amount of Si and Cu concentration in the alloy.
2. Within the 570÷555 ºC the eutectic mixture of Si and α-aluminum forms, leading to a further localized increase in Cu content of the remaining liquid. The Fe rich phases can also precipitate in this temperature range.
3. At approximately 540 ºC the Mg_2Si and $Al_8Mg_3FeSi_6$ phases begin to precipitate.
4. A reduction in the temperature allows for precipitation of Al_2Cu and $Al_{15}Mg_8Cu_2Si_6$ phases between 500÷470 ºC.

A comprehensive understanding of the solidification processes of the investigated industrial grade alloys requires the addition of grain refiners and eutectic Si modifiers using elements like: Ti, B, Sr, Na, Sb. Grain refiners that affect the morphology of the nucleating grains . Commercial aluminum alloys contain a limited number of active nucleating particles. In addition, these particles have a poor nucleating potency, therefore the melt requires a high degree of undercooling ($\Delta T_{DN} \approx 3 \div 5$ ºC, Figure 2) before these particles become active [4, 6]. Therefore, the effective melt processing requires the addition of grain refiners like the Al 3%Ti, 3%B master alloy. This master alloy contains a large number of insoluble boride particles, which effectively nucleate a great number of aluminum grains. Grain refiners added to the melt produce changes in the following thermal characteristics:

- The nucleation occurs far above the bulk equilibrium temperature T_L, for the liquidus temperature for alloys without grain modifiers (please refer to Figure 2).
- There is no undercooling before the actual growth temperature is reached (the recalescence effect is not present, $\Delta T_R \approx 0$ ºC, see Figure 2) [1, 10, 11].

Si modifiers (Sr, Na and Sb just to mention the most popular ones) change the morphology of the eutectic silicon crystals from large flakes into fibrous structures resembling a coral like morphology. The growth process of the eutectic silicon crystals is influenced by these additions, and the α+β eutectic reaction temperature is lowered by 5÷10ºC [1, 10].

2. Experimental conditions

The experimental alloy used in this investigation was prepared at the University of Windsor (Canada) in the Light Metals Casting Laboratory, by mixing the AC AlSi5Cu1(Mg) (C 355.2) commercial alloys and two master alloys AlSi49 and AlCu55, in a 10 kg capacity ceramic crucible. The melted test samples were held for 12 hours in Lindberg^{TM} electric resistance furnace at 850±5 ºC under a protective argon gas atmosphere. Before casting the melts were homogenized and degassed with the aim to reduce the hydrogen level below 0.100±0.005 ml H_2/100g of aluminum and the surface was carefully skimmed. A total of 24 samples of the AC AlSi9Cu alloy were prepared and their chemical compositions was analyzed by Optical Emission Spectroscopy (OES) as per the ASTM E1251 specification. The chemical compositions of this alloys is given in Table 2.

Table 2
Average chemical composition (wt %) of investigated alloy, equilibrium liquidus temperature - T_L and cooling rate – CR applied in the investigation,

Si	Fe	Cu	Mn	Mg	Zn	Ti	T_L, [ºC]	CR, [ºCs^{-1}]
9,09	0,18	1,05	0,38	0,27	9,09	0,09	600	0,16
								0,48
								1,04

Thermal analysis (TA) tests were conducted using the UMSA Technology Platform [15] developed at the University of Windsor in collaboration with the Silesian University of Technology.

The TA test samples were cast into a 0,25mm thick stainless steel cap. The cup was isolated at the top and bottom to allow for Newtonian type heat transfer only. A schematic of the experimental set-up for thermal analysis is depicted in Figure 1. In order to obtain statistical confidence, the TA experiments were repeated eight times for each time.

The cooling curve parameters considered in this work schematically depicted in Figure 2.

The aluminum dendritic network nucleation temperature – T_{DN}, the α+β eutectic nucleation temperature – $T_{E(Al+Si)N}$, the temperature where the new dendritic crystals have grown – T_{Dmin}, the temperature where the new silicon crystals have grown – $T_{E(Al+Si)min}$, were calculated using the first derivative of the cooling curve [3, 5].

The UMSA test analysis samples were cut longitudinally and then sectioned horizontally approximately 15 mm from the bottom and were prepared for metallographic analysis using standard procedures. Metallographic specimens were etched using 0.5% HF and a Keller & Dix etching solution [14].

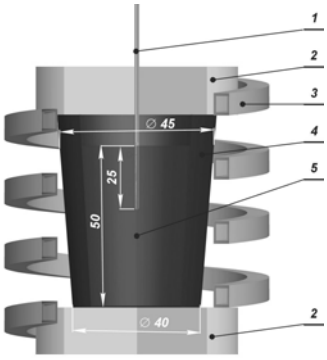

Fig. 1. Schematic of the UMSA Thermal Analysis Platform experimental set-up: 1 – low thermal mass thermocouple, 2 – thermal insulation, 3 – heating and cooling coil, 4 – steel cup, 5 – test sample

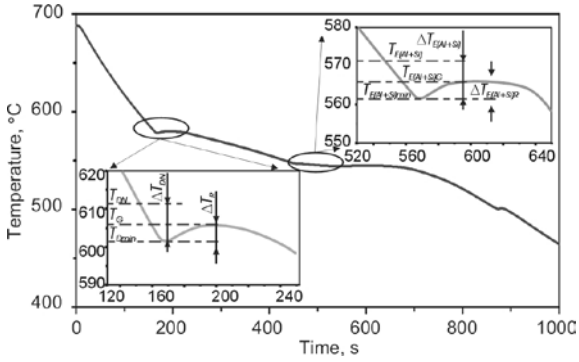

Fig. 2. Generic AC AlSi9Cu alloy cooling curve obtained under the authors non-equilibrium experimental, T_{DN} – aluminum dendritic network nucleation temperature, $T_{E(Al+Si)}$ – equilibrium eutectic temperature, T_{Dmin}, $T_{E(Al+Si)min}$- temperature where the newly nucleated crystal has grown, ΔT_{DN}, $\Delta T_{E(Al+Si)N}$ nucleation undercooling, ΔT_R, $\Delta T_{E(Al+Si)R}$ recalescence temperature

For comprehensive characterization of the Si structures a Leica Q-Win™ and a Simagis Research™ Image Analysis System were utilized. The morphology of the sectioned Si particles was characterized by the average area, average perimeter and equivalent diameter while the shape of the Si particles was determined by the aspect ratio and by the circuit factor. The shape and size characterized parameters were used to the Silicon Modification Level (SML) determination. Image Analysis procedures were developed for rapid determination of the parameters, which characterize the size and shape of the Si particles. SML was evaluated by Artificial Neural Network (ANN), which acquired knowledge during the learning process based on the shape and size characterized parameters acquired from the AFS Chart [12, 13].

3. Results and discussion

The cooling curves recorded for AC AlSi9Cu alloy at various cooling rates are shown in Figure 3. It is seen that formation temperatures of the various phases are changed when the cooling rate is increased. The shift magnitude increases with an increasing cooling rate. This shift changes the characteristic parameters of thermal analysis particularly in the liquidus region.

The cooling rate is proportional to the heat extraction from the sample during solidification. Therefore, at a low cooling rate (0.16 ºC·s^{-1}), the rate of heat extraction from the sample is slow and the slope of the cooling curve is small. So, it creates a wide cooling curve. But, at a high cooling rate (1,04 ºC·s^{-1}) the rate of heat extraction from the sample is fast, the slope of the cooling curve is steep and it makes a narrow cooling curve.

Figure 4 shows the variation of the aluminum nucleation temperature as a function of cooling rate and the variation of the Al nucleation undercooling and recalescence temperature. It is evidence from the plot, that the Al nucleation temperature increase with increase cooling rate from 0,16 to 1,04 ºC·s^{-1}, the Al nucleation temperature increases from 586,55 to 605,75°C.. Increasing the cooling rate increases the heat extraction. Therefore, the melt is cooled to a lower temperature than the equilibrium melting point. Due to the increase the cooling rate the nucleation undercooling increase. The phenomena of an increase in the nucleation temperature with an increase in the solidification rate depends on the mobility of the clusters of atoms in the melt. These groups of the froze atoms produces the fluctuation clusters and fluctuation embryos, which are the nucleation primers. The increase of the cooling rate with an increase amount of the nucleation primers and reduction of the recalescence temperature is well established fact. This effect have influence on the grain size. Figure 5 shows the variation of the grain size and secondary dendrite arm spacing as a function of cooling rate. As seen on the picture the increase cooling rate decrease strongly the grain size and SDAS.

The variation of SADAS (secondary dendrite arm spacing) has been showed graphically in Figure 5. SDAS is stricte depending on the cooling rate. In the highest cooling rate, the SDAS is fine (≈26,6 μm) and easily visible. For the sample that was cooled with lowest cooling rate, the SDAS is large (≈79,06 μm). Therefore the alloy's design and process engineers have a wide range of solidification rates (process parameters) to chose from.

Mechanical properties of the aluminum alloys are strongly dependent on the effect of SDAS. Tensile properties increase with a decrease the SDAS. Investigations results shows, the increase the cooling rate from 0,16 ºC·s^{-1} to 1,04 ºC·s^{-1}influance on the reduction of the SDAS, what have influence on the ultimate tensile strength (UTS). The UTS increase from 252 MPa for lowest cooling rate to 267 MPa for highest cooling rate (Figure 5).

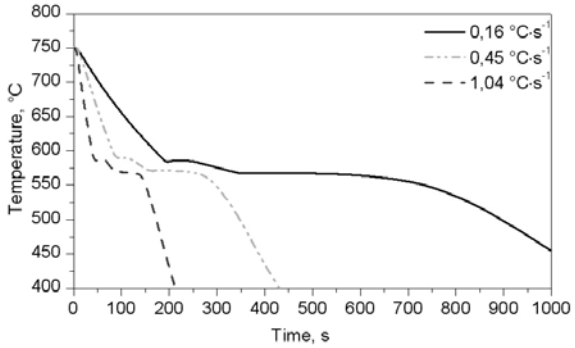

Fig. 3. Cooling curves of AC AlSi9Cu alloy at various solidification conditions.

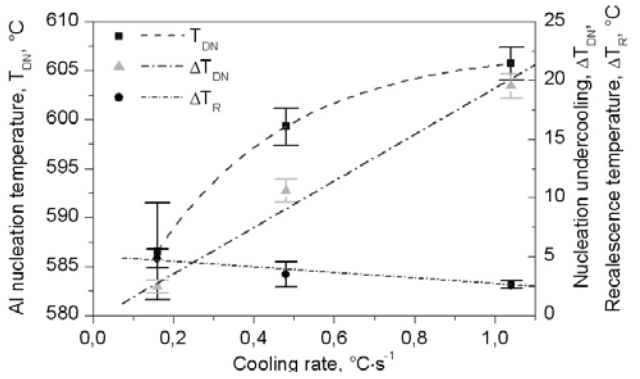

Fig. 4 Variation of the Al nucleate temperature as a function of cooling rate and variation of the Al nucleate undercooling and recalescence temperature as a function of cooling rate

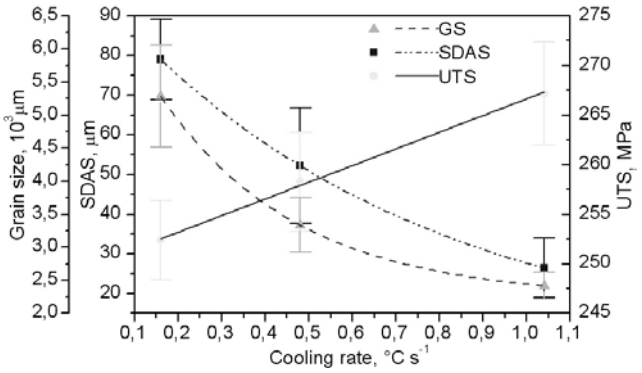

Fig. 5. Variation of the grain size SDAS and UTS as a function of cooling rate

4. Conclusions

The results are summarized as follows:

1. Solidification parameters are affected by the cooling rate. The formation temperatures of various phases are changed with an increasing cooling rate.
2. Increasing the cooling rate increases significantly the Al nucleate temperature, nucleation undercooling temperature, solidification range and decreases the recalescence undercooling temperature. These phenomena lead to an increased number of nucleus that affect the size of the grains and the Secondary Dendrite Arm Spacing (SDAS).

References

[1] J.G. Kauffman, E. L. Rooy: Aluminum Alloy Castings, ASM International, Ohio 2005.
[2] S.G. Shabestari, M. Malekan: Thermal Analysis Study of the Effect of the Cooling Rate on the Microstructure and Solidification Parameters of 319 Aluminum Alloy, Canadian Metallurgical Quarterly, Vol 44, 2005.
[3] L.A. Dobrzański, W. Kasprzak, J Sokołowski, R. Maniara, M. Krupiński: Applications of the derivation analysis for assessment of the ACAlSi7Cu alloy crystallization process cooled with different cooling rate, COMMENT 2005, Proceedings of the 13th International Scientific Conference, Gliwice-Wisła, 2005.
[4] L.A Dobrzański, K. Labisz, R. Maniara: „Microstructure investigation and hardness measurement in Al-Ti alloy with additions of Mg after heat treatment", COMMENT 2005, Proceedings of the 13th International Scientific Conference, Gliwice-Wisła, 2005.
[5] R. MacKay, M. Djurdjevic, J. H. Sokolowski: The Effect of Cooling Rate on the Fraction Solid of the Metallurgical Reaction in the 319 Alloy, AFS Transaction, 2000.
[6] C. H Cáceres, M. B. Djurdjevic, T. J. Stockwell, J. H. Sokolowski: Cast Al: The Effect of Cu Content on the Level of Microporosity in Al-Si-Cu-Mg Casting Alloys, Scripta Materiala, 1999.
[7] J. M. Boileau, J. W. Zindel and J. E. Allison: The Effect of Solidification Time on the Mechanical Properties in a Cast A356-T6 Aluminum Alloy, Society of Automotive Engineers, Inc., 1997.
[8] A. M. Samuel, A. Gotmare, F. H. Samuel: Effect of Solidification Rate and Metal Feedability on Porosity and SiC/Al_2O_3 Particle Distributing in an Al-Si-Mg (359) Alloy, Composite Science and Technology, 1994.
[9] L. Bäckerud, E. Król, J. Tamminen: Solidification Characteristics of Aluminum Alloys, Vol. 1, Universitetsforlaget, Oslo, 1986.
[10] L. Bäckerud, G. Chai, J. Tamminen: Solidification Characteristics of Aluminum Alloys, Vol. 2., AFS, 1992.
[11] L. Bäckerud, G. Chai: Solidification Characteristics of Aluminum Alloys, Vol. 3, AFS, 1992.
[12] American Foundry Society, (AFS): Chart for Microstructure Control in Hypoeutectic Aluminum Silicon Alloys, American Foundry Society, Inc., Des Plaines, Illinois.
[13] Modification rating System for Structure of Hypoeutectik Aluminium Silicon Casting Alloys, KBI Aluminium Master Alloys Product Literature.
[14] K. Radhakrishna, S. Seshan and M.R. Seshadri: Dendrite Arm Spacing in Aluminum Alloy Casting, AFS Transactions, Vol. 88, 1980.
[15] http://www.uwindsor.ca/umsa.